International Journal of Scientific Engineering and Research (IJSER)
ISSN (Online): 2347-3878
SJIF (2024): 6.623

Signal Conditioning Circuit for Energy Harvesters

Srikanta S[1], Dr. K. P. Lakshmi[2]

[1]Department of ECE, BMSCE, Bengaluru, India
Email: *srikanta.lvs22[at]bmsce.in*

[2]HOD, Professor, Department of ECE, BMSCE Bengaluru, India
Email: *kpl.ece[at]bmsce.ac.in*

Abstract: ***In today's fast-paced world of science and technology, efficient utilization of energy resources is vital to address rising global demands while fostering sustainable development. Rapid industrialization and societal advancements have significantly increased energy consumption, driving the need for innovative solutions to harness unused energy from the environment. This work focuses on investigating, designing, and implementing methods to capture dissipated energy from electronic devices and industrial machinery, converting waste heat into usable electricity. The study highlights a signal conditioning circuit developed to harvest renewable energy in the form of heat, primarily from sources like server rooms, electronic devices, or industrial machinery where substantial heat is dissipated. The circuit features a resistive Wheatstone bridge in a balanced state, with one arm comprising a PT100 sensor. Temperature variations cause the bridge to become unbalanced, generating a small, low- amplitude, and noisy signal. To process this signal, an AD620 instrumentation amplifier is used, which amplifies it, reduces noise, and provides enhanced common-mode rejection and filtering capabilities. The AD620 module amplifies the signal to approximately 0.9V, sufficient to charge a 1V rechargeable cell. Additionally, an MCP1640 circuit boosts the voltage to a stable 3.3V DC. For battery safety, an MCP73831 IC acts as a charge controller, complemented by a PCM module for overcurrent and surge protection, ensuring secure storage in a rechargeable battery.***

Keywords: energy harvesting, waste heat recovery, signal conditioning, renewable energy circuits, thermal to electrical conversion

1. Introduction

In today's rapidly advancing technological world, achieving sustainable development goals is paramount. With the ever-increasing demand for energy and a global shift towards environmentally friendly solutions, energy harvesting has emerged as a key area of innovation. The principle of energy conservation, as stated by Julius Robert Mayer's law "Energy can neither be created nor destroyed; it is merely converted from one form to another" guides this movement towards harnessing energy that would otherwise be wasted.

[1] designed an energy management design guide for self-powered sensors which shows even the smallest amounts of energy dissipated into the environment have the potential to be captured and repurposed to fulfill human energy needs.

A large portion of energy harvested today comes from renewable sources such as solar, wind, geothermal, tidal, and seismic waves. These sources are abundant, naturally recurring, and offer significant advantages in terms of environmental sustainability. However, there are also numerous opportunities to capture energy from less conventional sources, including those generated by human-made devices and processes. Thermal energy from devices like smartphones or laptops, heat dissipated in server rooms, vibrational energy from industrial machinery, and even ambient electromagnetic waves are all viable sources of energy that can be harvested and converted into useful electrical power. Heat driven from human body is received by thermoelectric generators can be used to power watch like wearable devices [2].

Energy harvesting technologies allow us to take advantage of this ambient energy. For example, temperature changes in electronic devices such as laptops and smartphones result in heat dissipation, which can be captured using temperature sensors like thermocouples or resistance temperature detectors (RTDs). In server rooms, where vast amounts of heat are released, there is significant potential for energy recovery. By capturing this heat and converting it into electrical energy through a signal conditioning circuit, we can utilize energy that would otherwise be wasted, contributing to the overall efficiency of our power systems.

The signal conditioning circuit is vital as it processes the raw energy captured by the harvester, amplifies and stabilizes the voltage, and ensures that it is suitable for powering electronic devices or sensors. These self-powered systems, powered by renewable sources, present a sustainable, autonomous solution for energy harvesting. In fast forward generation, the efficient management of heat generated by electronic devices, server rooms, and electrical machines is crucial. The inevitable heating effect in these environments can significantly impact the performance and longevity of equipment, necessitating sophisticated monitoring and management solutions. One effective method for detecting and quantifying this heat involves the use of the PT100 Resistance Temperature Detector sensor as shown in Fig 1.7. An RTD is a passive device used for measuring temperature, functioning based on the principle that a metal's resistance varies with temperature.

Figure 1: PT100 Resistance Temperature Detector

Platinum sensor elements as shown in Fig.1., crafted from pure platinum wire, exhibit a positive temperature coefficient. Their remarkable linearity and long-term stability render them highly precise sensors for harvesting energy and industrial applications. These platinum RTD elements are compatible with copper wire extension leads and are ideal for industrial settings demanding stability and linearity across a broad

Platinum sensor element, crafted from pure platinum wire, exhibit a positive temperature coefficient.

The remarkable linearity and long-term stability render them highly precise sensors. These platinum RTD elements are compatible with copper wire extension leads and are ideal for industrial settings demanding stability and linearity and hence the signal conditioning circuit.

In many applications, raw sensor outputs are small, noisy, or not within the appropriate range for signal conditioning. The role of the signal conditioning circuit is to ensure that these signals are clean, accurate, and robust enough for reliable interpretation. The selected sensor has a wide range of temperature from -50°c to +250°c.

Table 1: PT100 Temperature and resistance table

Temperature in °C	Resistance in Ω	Temperature in °C	Resistance in Ω
37	115.88	68	123.39
38	116.013	69	123.98
39	116.24	70	124.38
40	116.38	71	124.7
41	116.59	72	125.05
42	116.77	73	125.35
43	116.968	74	125.65
44	117.13	75	126.06
45	117.4	76	126.47
46	117.58	77	126.88
47	117.69	78	127.37
48	117.8	79	127.8
49	118.16	80	128.39
50	118.317	81	128.9
51	118.67	82	129.35
52	118.94	83	129.97
53	119.23	84	130.51
54	119.45	85	131.28
55	119.6	86	131.69
56	119.81	87	132.2
57	120	88	132.59
58	120.53	89	132.97
59	120.7	90	133.32
60	120.9	91	133.67
61	121.21	92	133.85
62	121.56	93	134.07
63	121.86	94	134.34
64	122.24	95	135.148
65	122.65	96	136.04
66	122.9	97	136.97
67	123.15	98	137.54

The table 1. illustrates the behavior of the PT100 RTD, which demonstrates how the resistance of platinum material changes as the temperature varies. This change in resistance is a defining characteristic of PT100 sensors, making them highly reliable for temperature measurement.

Linear Relationship: The resistance increases linearly with a rise in temperature. This linearity ensures that changes in temperature can be directly correlated to changes in resistance, allowing for precise and predictable readings.
Range of Data: The table captures specific resistance values for corresponding temperature points within a given range.

Sensitivity: The PT100 sensor is designed to be highly sensitive, with resistance increasing steadily as the temperature rises. This sensitivity allows it to detect even minor temperature changes, which is crucial in industrial and scientific applications.

The table 1. essentially serves as a calibration guide, enabling to interpret resistance measurements and convert them into accurate temperature readings for various applications.

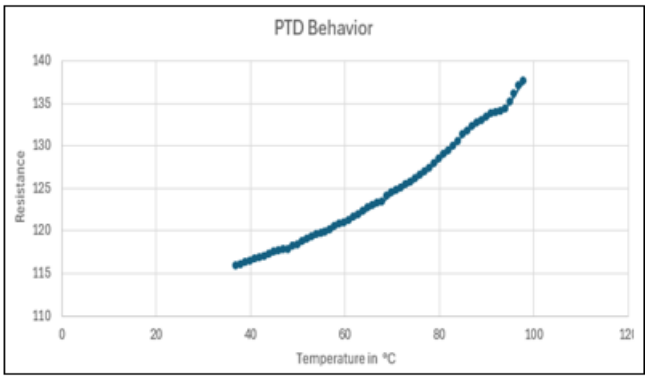

Figure 1 (a): PT100 Resistance Temperature Detector

The graph in the figure 1a. depicts the behavior of a Platinum Temperature Detector i.e, PTD, showing the relationship between temperature in °C and resistance in ohms.

Positive Correlation: The graph clearly indicates that as the temperature increases, the resistance also increases. This is a characteristic feature of platinum sensors like PTDs, which are designed to exhibit predictable resistance changes with temperature.

Gradual Rise: Initially, the resistance increases steadily with temperature. This linear-like behavior ensures accurate temperature readings across the lower range.

Slight Non-Linearity at Higher Temperatures: As the temperature reaches the higher end of the scale, the resistance continues to rise, but the slope of the graph may slightly change. This suggests that while the PTD maintains a reliable trend, minor nonlinearities could emerge due to material properties or measurement conditions.

Sensitivity: The graph's steep upward trend demonstrates the sensor's high sensitivity, capable of detecting even small temperature variations by registering corresponding resistance changes.

The graph in the Fig 1a. reinforces the PTD's utility as a precise and stable tool for temperature measurement, particularly in environments demanding high accuracy and reliability.

Signal Conditioning Circuit:

A signal conditioning circuit is a critical electronic system designed to convert, modify, and optimize signals from sensors or transducers into a format suitable for further processing, analysis, or display. In many applications, raw sensor outputs are weak, noisy, or not within the appropriate range for data acquisition systems or controllers. The role of the signal conditioning circuit is to ensure that these signals are clean, accurate, and robust enough for reliable interpretation. The proposed Signal conditioning circuit shown below is designed by keenly observing the behavior of the circuit through various simulation platforms loke NI-Multisim and simulated.

Pre-phase of the work underwent on finding the problem, understanding the stages of the process and simulating the circuit stages to understand the behavior of the waveforms and output. Selecting an amplifier requires careful consideration of several key factors, especially when dealing with signals of very low amplitude, such as those in the millivolt range. It's crucial to choose an amplifier that offers high accuracy and precision to ensure the signal is amplified to a higher voltage level without distortion. With this the amplifier should incorporate effective noise filtering to maintain signal integrity, as unwanted noise can severely affect low-amplitude signals. Another important criterion is the amplifier's Common-Mode Rejection Ratio (CMRR), which should be high to minimize interference from external noise sources. Low power consumption is essential to ensure efficiency, especially in applications where power resources are limited. This combination of attributes ensures optimal performance in sensitive signal amplification tasks which tends to accurate amplification of captured low-level signals.

2. Methodology

Signal conditioning circuit in energy harvesting energy follows a structured approach to capture, condition, and store energy derived from ambient energy sources. The system is composed of several stages, each playing a crucial role in converting ambient energy into usable electrical energy stored in a battery. The block diagram Fig. 2 helps in visualizing the flow of energy through different stages:

Figure 2: Block Diagram

a) ***Ambient energy capture*:** Ambient energy, in the form of heat, is transformed into low-level electrical signals using a PT100 temperature sensor, which functions as a key component in energy harvesting systems. Ambient energy in the form of heat generated by electronic gadgets, such as a Raspberry Pi processor and a laptop, is captured using a PT100 temperature sensor. The PT100 is a precision resistance temperature detector (RTD) that changes its resistance with temperature, making it highly sensitive and accurate for detecting heat in both scenarios. By converting heat from ambient sources into electrical signals, the PT100 enables efficient energy harvesting, providing a reliable low-amplitude signal output that can be processed and utilized for various applications, such as powering low-energy devices or further energy storage.

1) ***Heat Sensing on Raspberry Pi Processor**:* In the first case as shown in the Fig. 3, the PT100 sensor is placed near the Raspberry Pi processor, which generates heat during operation.

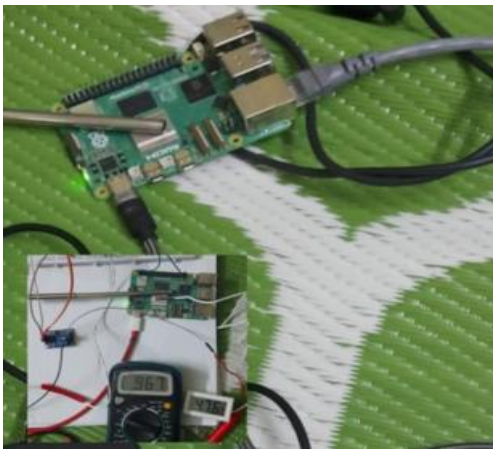

Figure 3: PTD on Raspberry-pi processor

As the processor runs computational tasks, its temperature rises due to the power consumption and processing load. The PT100 sensor captures this increase in temperature by sensing the heat emitted from the processor's surface. The heat is translated into a change in resistance in the PT100, and through a connected Wheatstone bridge circuit, this resistance variation is converted into a small voltage signal. This signal is then amplified and processed in the later stages of the circuit. The measured temperature data from the Raspberry Pi processor provides valuable information on thermal management and energy harvesting from waste heat generated during computation.

2) ***Heat Captured from a Laptop:*** In this case, the PT100 sensor is placed near a laptop's heat-emitting surface, such as the processor or exhaust vents, where significant amounts of heat are produced during extended usage. Laptops generate a considerable amount of heat as they handle tasks like multitasking, media playback, and

high-performance computing. Like the first case, the PT100 detects the temperature rise from these components, causing a change in its resistance.

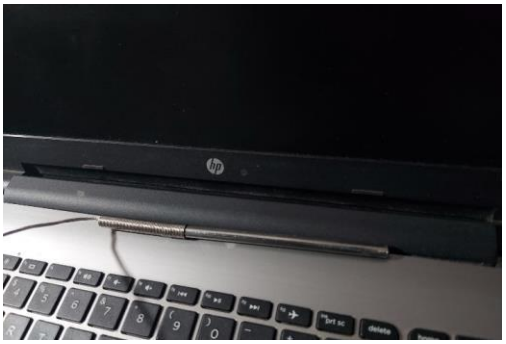

Figure 4: Sensor placed on the Laptop

The resistance variation is again processed using a Wheatstone bridge, followed by amplification and conversion of the small signal into a usable voltage output. This enables the system to capture and analyze the heat energy produced by the laptop, showing how energy from such devices can be harnessed in the form of heat.

b) ***Wheatstone Bridge:*** A Wheatstone bridge circuit is a fundamental configuration used for precise measurement of electrical resistance. In a balanced Wheatstone bridge, the circuit comprises four arms. One arm incorporates a PT100 RTD, while the other three arms consist of fixed resistors. The PT100 RTD, known for its accuracy in temperature measurement, exhibits a resistance that varies predictably with temperature. When the bridge is balanced, the voltage across the bridge's midpoint is zero, indicating that the ratios of the resistances in the two halves of the circuit are equal.

In the signal conditioning process, the Wheatstone bridge plays a pivotal role in translating the small electrical signals harvested from ambient energy into a more usable form. The Wheatstone bridge is used here to detect these minute resistance variations effectively. The voltage output from the Wheatstone bridge is then prepared for the next stage of amplification, ensuring that even small ambient changes can be accurately captured and processed for further applications.

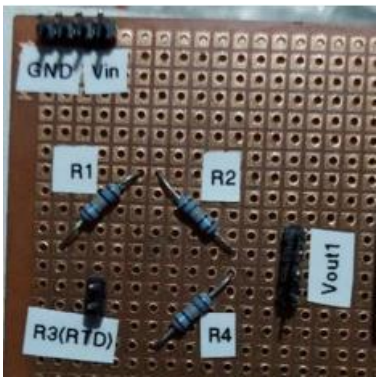

Figure 5: Wheatstone bridge

In the signal conditioning circuit, the Wheatstone bridge in Fig. 5 configuration plays a crucial role in detecting temperature variations using the PT100 sensor. The Wheatstone bridge consists of four resistive arms, resistances R1, R2, R3, and R4 as shown in the Fig. 5. In this configuration, the values of the resistances are as follows:

R1 = 112.4 Ω, R2 = 112.4 Ω, R3 = 112.2 Ω, and R4 = 112.4 Ω. Notably, the PT100 sensor forms the R3 arm of the bridge for which header pins are allotted so that PT100 can be connected which completes a balanced Wheatstone bridge setup. It is observed that at 24°C room temperature, resistance of PT100 is 112.2 Ω.

The bridge is initially balanced at the room temperature, which means that the voltage across the bridge is ideally zero or very close to zero, as the voltage drops across the two halves of the bridge R1-R2 and R3-R4 are equal.

c) ***Instrumentation Amplifier:*** The AD620A module often provides superior performance over the AD623 IC due to its lower input offset voltage, higher CMRR, and lower noise characteristics, making it ideal for precise, low-noise applications. AD620A modules are typically configured with well-designed PCB layouts that reduce noise and interference, in contrast to breadboard implementations of the AD623, which may suffer from parasitic effects. This design advantage results in a more stable and accurate amplification, making the AD620A particularly suitable for high-sensitivity measurements where signal integrity is critical.

The AD620 instrumentation amplifier module is created to boost faint AC or DC signals, usually from analog sensors, strain gauges, transducers, or equivalent devices. This module shown in the fig. 6, is particularly beneficial for amplifying weak signals accurately for subsequent processing or measurement tasks.

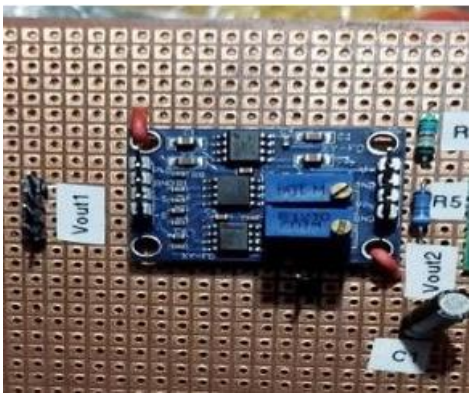

Figure 6: AD620A circuitry

The core component of the module is the AD620A, a built-in instrumentation amplifier. This specific integrated circuit is recognized for its capability to offer precise and steady amplification, making it suitable for tasks that need high accuracy and minimal noise.

The key reasons for choosing the AD620 was its high accuracy and linearity. The maximum nonlinearity is limited to 40 ppm, ensuring that the output signal remains proportional to the input over a wide range of conditions. The low offset voltage of 50 µV max and minimal offset drift of 0.6 µV/°C max make the AD620 suitable small signal amplification. These characteristics minimize errors and ensure accurate signal generation, even in environments

where temperature fluctuations occur. The AD620 also boasts low noise characteristics, with an input voltage noise of 9 nano volts per hertz at 1 kHz and 0.28 µV p-p in the 0.1 Hz to 10 Hz band. This low noise performance is essential for precise applications, where small signal amplification from the Wheatstone bridge is required without introducing significant noise into the system.

The second op-amp within the LM358 is also utilized as a unity gain buffer to provide a stable reference voltage to the AD620. Maintaining a consistent Vref is critical for the accurate operation of the AD620, as it determines the baseline for the amplified output signal. By using the LM358 to buffer the Vref, any fluctuations in the power supply or other parts of the circuit are minimized, ensuring that the AD620 operates with maximum precision. The input to the LM358 is controlled by a 10K potentiometer.

The AD620 module can accept input signals ranging from 100 µV to 300 mV, which can be applied to the S+ and S- pins. For a ground-referenced or single-ended signal, the input is connected to S+, while S- is tied to ground. Alternatively, the module can accommodate differential signals from sources like bridge sensors, which connect across the S+ and S- pins.To ensure safe operation and protect the internal components, a 1K series resistor is employed at the inputs to limit the current. The gain of the AD620A is adjustable via a 100K potentiometer, allowing for a gain range from 1.5x to 1000x. Lower resistance settings correspond to higher gain, with clockwise rotation of the potentiometer increasing the gain.

The amplified output from the AD620 is fed into one of the two LM358 op-amps, which are configured as unity gain buffers. The LM358 is capable of sourcing approximately 30 mA and sinking about 20 mA, ensuring sufficient output drive capability. The buffered output is available on the pin labeled VOUT, providing a stable signal for further processing. The provided diagrams illustrate the basic connection setups for both single-ended and differential inputs, along with the configuration for adjusting the zero offset.

By utilizing the AD620A, the module achieves high precision and versatility in signal conditioning applications, making it suitable for a wide range of measurement and data acquisition tasks and signal conditioning as well.

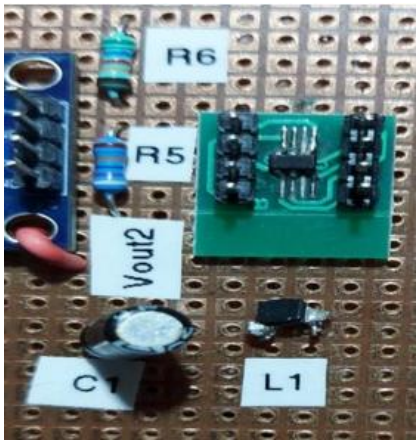

Figure 7: MCP1640 Boost converter

d) ***Boost Converter:*** A boost converter is a type of DC Chopper designed to increase the low input voltage to a higher output voltage, making it essential in systems where energy harvesters generate low-power signals. In the context of this work, the MCP1640 boost converter has been chosen due to its efficiency, compact size, and ability to operate at low input voltages, making it ideal for energy harvesting applications.

The MCP1640 steps in by taking the low voltage signal and efficiently boosting it to the desired level. In this design, it is to step up the voltage to at least 3.3V, which is suitable for storing in a battery or powering other components. The MCP1640 is capable of boosting voltages even from as low as 0.65V, which makes it highly suitable for energy harvesters that generate minimal output. The boost converter is equipped with features such as a low-resistance N-channel boost switch and a synchronous P-channel switch, which reduce power losses and improve overall efficiency.

MCP1640 integrates necessary compensation and protection circuitry, minimizing the need for external components and simplifying the design. This results in a compact circuit that not only boosts the voltage but also protects the system from potential faults like overvoltage or undervoltage conditions. By ensuring a stable and boosted output, the boost converter plays a critical role in ensuring the energy harvester's low-level electrical signals can be transformed into usable power for charging a 3.3V battery and powering the overall system efficiently. Thus, in the overall methodology, the boost converter acts as the bridge between the amplified low-level signal and the energy storage system, making sure the energy harvested and conditioned through previous stages is effectively utilized. Partially the the energy storage is successful but the boosting upto 3.3V was possible but the interruption caused over zero PCB is one of the care to be taken. A printed circuit board of this design can be helpful to overcome this effect. MCP1640 DC-DC step-up boost converter is chosen specifically for its ability to efficiently manage power in a low-voltage, battery-operated environment. MCP1640 played a critical role by enabling efficient voltage boosting for various battery-powered devices, including wireless sensors, personal medical products, and portable instruments. Its ability to operate from low-voltage sources and deliver stable power output ensured the system could run efficiently across multiple applications, making it a versatile and indispensable component in the design.

The inductor enables energy storage and transfer, allowing the IC to step up the input voltage. In this design, a 4.7 µH inductor is connected between Pin 1 (SW) and Pin 6 (VIN). The inductor stores energy when the switch is closed and releases it when the switch opens, which enables the step-up conversion of voltage. The inductor's value of 4.7 µH is chosen to optimize efficiency and minimize current ripple, crucial for maintaining stable performance. It ensures that the converter can maintain the desired output voltage while managing the energy transfer between the input and output effectively. A voltage divider circuit is used for feedback control in the design. The resistors in the voltage divider allow the feedback pin to sense the output voltage and adjust the switching accordingly. The following resistors are used:

Resistance R5 in the circuit is 976 kΩ This resistor is connected between Pin 5 i.e., Vout 3 and Pin 4 i.e., FB. It serves as the upper resistor in the voltage divider, helping to step down the output voltage for feedback. Resistance R6 in the circuit is 562 kΩ. This resistor is connected between Pin 4 i.e., FB and ground. It forms the lower part of the voltage divider, working with R5 to scale the output voltage for feedback. The resistor values are the resistor values are chosen to achieve the desired feedback voltage, which regulates the output at 3.3V. The voltage divider ensures that the feedback pin accurately detects the output voltage, enabling the IC to make fine adjustments to maintain a stable output.

The problem with the boost converter is present, as per datasheet, input value ranges are matching and circuitry setup is also meeting its standards. Even though this stage is not obtaining results, the proper stable dc voltage of 0.9V is achieved and subsequently the protection circuits also meet providing desired functionality when tested individual stages

e) ***Charge Controller:*** A charge controller IC in a signal conditioning circuit is essential when the circuit is part of a battery-powered system, particularly for autonomous or remote sensor applications. Signal conditioning circuits, which process low-level signals from sensors, often operate in environments where access to a stable external power source is limited or impractical. The charge controller IC manages the charging of a rechargeable.

The MCP73831T-5ACI/OT as shown in Fig 8 is a highly integrated linear charge management controller designed for single-cell lithium-ion or lithium-polymer battery applications. It provides a simple and efficient charging solution with minimal external components. The IC operates as a fully programmable charger with a constant current and constant voltage regulation, offering protection features such as thermal regulation and overvoltage protection. It is commonly used in portable electronics, wearables, and small battery-powered devices. This work focuses on the configuration of the MCP73831T-5ACI/OT in a charging circuit as shown in Fig 8, detailing the pin assignments and the role of key external components.

An LED and a 470Ω resistor are connected between Pin 4 (VDD) and Pin 1 (STAT) to indicate the charging status of the battery. When the battery is charging, the STAT pin pulls low, causing the LED to illuminate, showing that the charging process is in progress. Once the battery is fully charged, the STAT pin goes high, and the LED turns off. The 470Ω resistor limits the current flowing through the LED to prevent damage, ensuring that the LED operates safely and reliably, provides a visual indication of the charging status, with the resistor ensuring safe current flow to the LED.

This resistor sets the charge current according to the formula:

$$I_{CHG} = \frac{1000}{R_{PROG}}$$

$$I_{CHG} = \frac{1000}{2K} = 500mA$$

battery e.g., Li-ion used to power the system, ensuring safe and efficient charging cycles. It prevents overcharging, which can damage the battery, reduce its lifespan, or create safety hazards, and it typically manages different charging stages, such as constant current and constant voltage phases, for optimized battery health. In low-power, energy-harvesting applications, the charge controller regulates the intermittent power coming from energy sources like solar panels, converting this energy into a stable and usable form to recharge the battery. By integrating a charge controller IC, the system can autonomously maintain a reliable power source, ensuring continuous operation of the signal conditioning circuit without user intervention.

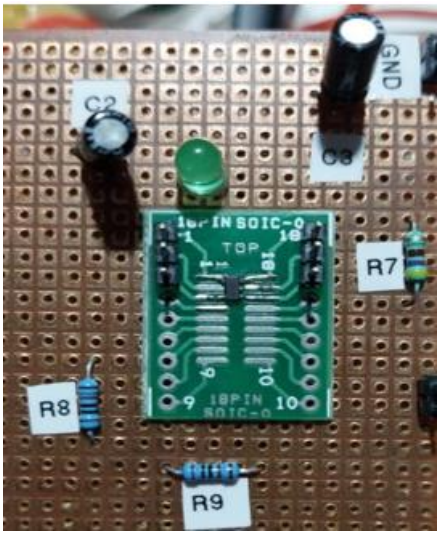

Figure 8: MCP73831 charge controller

For a 2kΩ resistor, the charging current is set to 500mA. The selected resistor value determines the safe and appropriate charging rate for the battery, balancing charging speed with the protection of the battery's lifespan. Additionally, a 4.7µF capacitor is placed near VBAT i.e. Pin 3, which is the output pin to the battery. This capacitor helps stabilize the voltage during charging, smoothing out any fluctuations or noise that may be present at the battery terminal. It ensures that the charging process is consistent, protecting both the battery and the IC from voltage spikes or irregularities. The capacitor Stabilizes the voltage at the battery terminal, ensuring a smooth and safe charging operation, and filters out any noise in the circuit and helps in filtering the output, improving overall charging performance and reliability.

f) ***Power Controller Module:*** A BatterySpace Protection Circuit for 3.6V/3.7V 18650 batteries is a vital component designed to safeguard Li-ion cells against overcurrent, surge current, overcharging, and over-discharging. This circuit continuously monitors the battery's voltage and current, ensuring it stays within safe operating limits. It typically includes a metal-oxide- semiconductor field-effect transistor and control circuitry. When an overcurrent or surge current event is detected, the circuit disconnects the load to prevent potential damage to the battery, such as overheating or internal short circuits. Additionally, it ensures the battery does not exceed its charge voltage limit or discharge below its safe minimum, enhancing its lifespan and safety. This circuit is widely used in applications like power tools, flashlights, and portable electronics to provide reliable battery protection and maintain performance integrity.

g) ***Battery:*** The 18650 lithium-ion battery, specified at 3.7V with a capacity of 2000mAh and energy rating of 7.4Wh, is a highly reliable choice for portable electronics due to its balance of power, compact size, and rechargeable capability. Designed with a cylindrical form factor with 18mm diameter and 65mm length, the 18650 cell is favored in applications requiring both high energy density and extended cycle life.

Figure 9: Rechargeable Battery

This battery type is engineered to deliver consistent, steady power output, making it suitable for devices that demand stable voltage over prolonged use. Its 2000mAh capacity allows for significant runtime, while the 7.4Wh energy rating highlights its efficiency in storing and supplying energy relative to its size. Notably, the 18650 batteries also include essential safety features, such as protection against overcharge, over-discharge, and short-circuiting, when combined with an appropriate protection circuit. These specifications make the 18650 an ideal power source for DIY projects, power tools, flashlights, and even electric vehicle battery packs, where compact power solutions are crucial.

Fig 10. below shows the design schematic of the signal conditioning circuit. The described setup features a Wheatstone bridge arrangement, where one of its arms incorporates a PT100 sensor. This sensor is known for its resistance-dependent sensitivity, making it a key component in precise measurements. Within the bridge, when there's a variation in resistance such as due to temperature changes in the PT100 sensor, a small differential voltage is generated across the bridge. To amplify this subtle signal, a custom-built instrumentation amplifier module utilizing the AD620 is employed. This module is enhanced with noise-removal capabilities to ensure accurate readings. The amplifier processes the signal, providing an output voltage in the range of 0.849 V to 0.951 V, as detailed in Table 2.

This amplified signal is then directed to a voltage- boosting circuit based on the MCP1640. The purpose of this stage is to elevate the signal voltage up to a stable 3.3 V level, suitable for further application. Following this, the boosted voltage passes through a charge controller integrated with a PCM18650-based battery management system. This system not only monitors and regulates the charging process but also ensures the safe storage of the obtained energy in a connected battery.Through these stages, the setup effectively translates a subtle physical parameter change detected by the PT100 sensor into a stored electrical charge, ready for practical use.

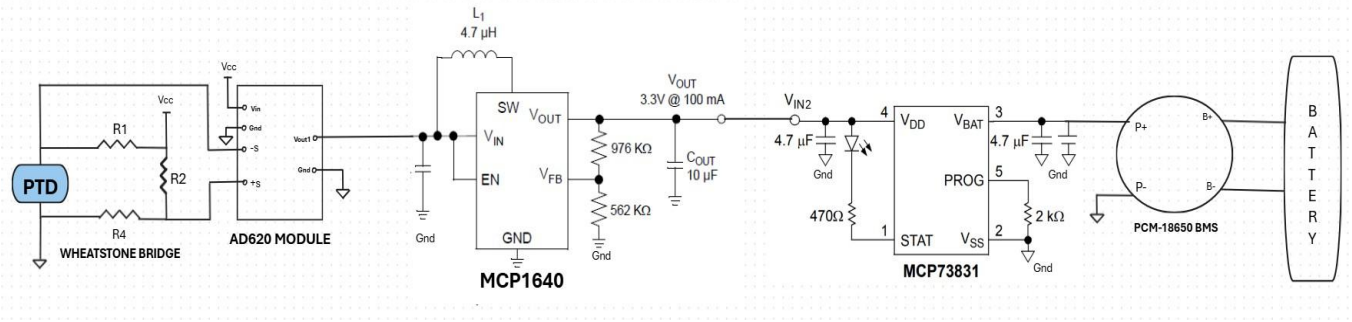

Figure 10: Signal conditioning circuit schematic

3. Results and Discussion

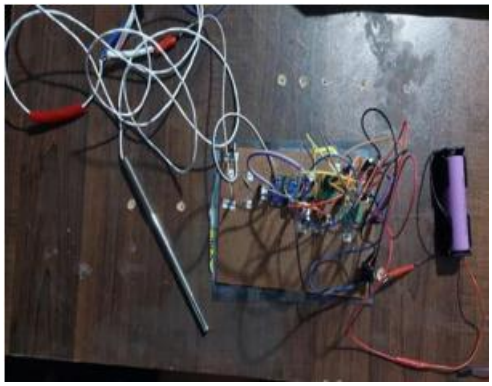

Figure 11: Proposed signal conditioning circuit

Each block in the methodology has great weightage in contributing for harvesting energy to a battery. By combining all the blocks whose functionality is tested, the integrated circuit of Signal conditioning circuit is as shown in above Fig. 11. The initial phase of the circuit is Vout1 which is the differential signal obtained through two nodes of the Wheatstone bridge which is named as s+ and s- nodes in the circuit. The graph below shown in Fig. 4 throws the light on the behavior of the sensor with variation in temperature parameter. The plot shown in below Fig 12 picturizes the exponential behavior of rise in voltage which is millivolt range. Temperature in °C on the x-axis against Voltage in mV on the y-axis. The original data points are represented by blue dots, while the fitted curve, following an exponential model. The practical results obtained as shown in the table. 2 are closer to the ideal expected behavior and the same output is passed to the AD620amplifier module for stepping up the voltage higher level.

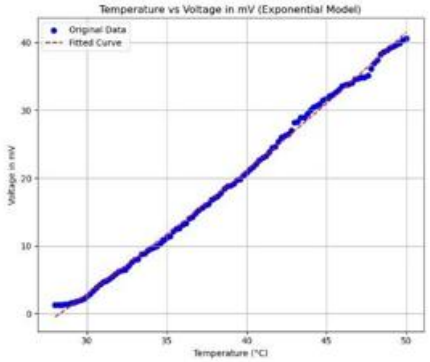

Figure 12: Wheatstone bridge output - Vout1

- The voltage and temperature increases correspondingly, following an exponential pattern, which is evident by the non-linear rise of the fitted curve.
- At lower temperatures from 25°C to 30°C, the increase in voltage is relatively gradual. As the temperature rises beyond 30°C, the voltage begins to increase more rapidly.

The fitted exponential model follows the trend of the original data points closely, especially at higher temperatures, confirming that the voltage increase accelerates with temperature.

The most important part of signal conditioning circuit is AD620A module. An AD620 is an instrumentation amplifier capable of capturing microvolt level voltage as well, AD620 is best suited for these types of applications. Th plot shown in below Fig 12 picturizes the linear behavior of the voltage which is closure to 1 volt range. Temperature in °C on the x-axis against Voltage in V on the y-axis. The practical results obtained as shown in the table 2 are closer to the ideal expected behavior which can be observed in table 1 and the same output is passed to the boost converter for stepping up the voltage to higher level.

- The voltage steadily increases with temperature from around 0.849 V at 27°C to approximately 0.951 V at 50°C.
- The original data points closely follow the fitted linear line, demonstrating a consistent and uniform increase in voltage with temperature.

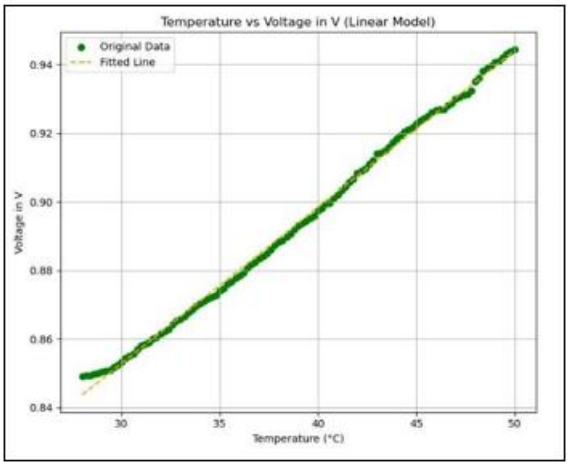

Figure 13: AD620 output – vout2

The Fig. 12 covers a smaller voltage range of 0 mV to 40 mV, while the Fig. 13 covers a range of 0.849 V to 0.951 V. This difference indicates that the exponential model captures more sensitive changes in voltage at the microvolt level, while the linear model demonstrates a more general trend over a larger voltage range. The choice between exponential and linear models depends on the intended use of the system. The exponential model may be more suitable for highly sensitive applications where fine voltage variations at higher temperatures need to be captured. On the other hand, the linear model is likely more appropriate for general-purpose applications where a straightforward temperature-voltage relationship is needed. Both graphs provide valuable insights into the relationship between temperature and voltage for the system being studied. The exponential model shows a rapidly increasing voltage response as temperature rises, indicating higher sensitivity at elevated temperatures. In contrast, the linear model demonstrates a proportional and steady voltage rise with temperature, offering simplicity and predictability in the system's behavior. Understanding these trends can help in optimizing the system for different temperature ranges and determining the most suitable model for specific applications in energy harvesting or temperature sensing technologies.

Table 2: voltage comparison table

Sl. No	Setup	Voltage in mV	Voltage in V
1	Simulation	77.418	1.013
2	Breadboard	19.9310	0.798
3	Zero PCB	11.5667	0.876

The table. 2 compares voltage readings across three setups at the room temperature: Simulation, Breadboard, and Zero PCB. In the Simulation setup, the measured voltage is 77.418 mV, corresponding to 1.013 V. On the Breadboard, the voltage measured is 19.9310 mV, resulting in 0.798 V. In the Zero PCB setup, the voltage is 11.5667 mV, translating to 0.876 V. These variations indicate differences in performance and potential losses or fluctuations across the setups, with the simulation yielding the highest initial voltage, followed by breadboard testing, and finally, the zero PCB setup showing a slight increase in output voltage despite a lower initial voltage measurement. This table shows the behavior of the circuit from simulation to PCB level which brings results close to real time

Table 3: Result table of Vout1 and Vout2

Temp in °C	Trial 1		Trial 2	
	Voltage in mV	Voltage in V	Voltage in mV	Voltage in V
27	2.7575	0.899	0.1133	0.849
29	3.5216	0.851	0.1599	0.85
30	5.4483	0.858	1.0882	0.853
31	7.8601	0.863	2.3968	0.855
32	9.1941	0.867	6.8171	0.864
33	11.1291	0.872	8.5644	0.869
34	13.251	0.875	10.296	0.874
35	13.251	0.875	12.0688	0.879
36	16.8438	0.884	14.1765	0.883
37	18.2885	0.889	16.5634	0.888
38	20.9963	0.895	17.8622	0.892
39	22.7769	0.900	19.774	0.897
40	25.2754	0.905	22.1709	0.902
41	27.7886	0.91	24.1954	0.907
42	30.1784	0.916	26.1127	0.913
43	32.4183	0.922	28.8618	0.917
44	35.0818	0.927	30.5641	0.922
45	36.7789	0.932	32.4209	0.926

46	38.3298	0.936	34.7255	0.931
47	38.7996	0.937	36.5754	0.936
48	42.0738	0.945	38.9531	0.941
49	43.9495	0.950	40.6355	0.945
50	43.6805	0.950	42.9348	0.951

The data presented in the table. 3 represents two trials conducted using the designed signal conditioning circuit, which processes the Wheatstone bridge output Vout1 and AD620 output Vout2. Readings are taken as Each trial correlates the output voltage with variable temperature gradients ranging from 27°C to 50°C. The results include:

Trial 1: The Wheatstone bridge output in millivolts and the circuit's output voltages Vout1 are observed to have a consistent increase with temperature. The bridge output begins at 2.7575 mV at 27°C and increases to a peak of 43.6805 mV at 50°C. Simultaneously, the circuit output Vout1 progresses from 0.899V to 0.950V, demonstrating a stable linear behavior.

Trial 2: Similar observations are made, with the bridge output starting at a lower 0.1133 mV at 27°C, peaking at 42.9348 mV at 50°C. The Vout1 values range from 0.849V to 0.951V, closely mirroring the trend seen in Trial 1 but with slight variations in the millivolt values.

The increase in the bridge output and Vout1 with temperature indicates that the circuit's sensitivity to temperature changes is reliable and consistent across trials, although some differences in output are evident due to potential variability in circuit components or environmental factors.

The graph below in Fig. 14 is combined version of all trials and readings, compares the output voltage Vout1 and Wheatstone bridge output for both trials against the temperature gradient. The graph demonstrates the linear increase of bridge output voltage in millivolts across the temperature range. The slight offset between the two trials, particularly at lower temperatures, with Trial 1 generally providing higher millivolt readings than Trial 2. The closely matching Vout1 behavior between both trials, emphasizing the circuit's consistent performance.

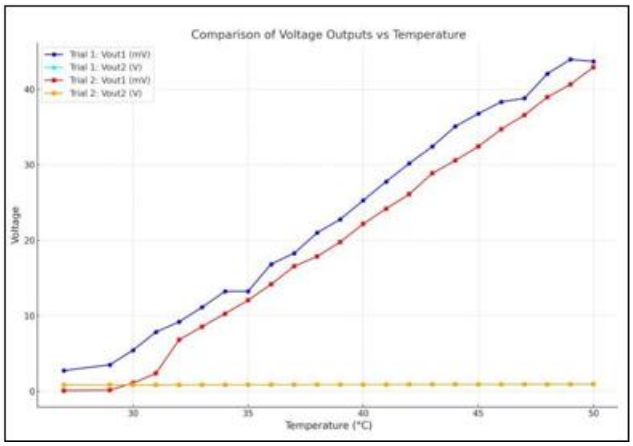

Figure 14: voltage graph derived from table 2.

Here is the corrected graph comparing the output voltages Wheatstone bridge output Vout1 in millivolts and Vout2 in volts from both trials across the temperature gradient. The graph illustrates the linear relationship and consistent performance of the circuit across the two trials, with slight deviations in the Wheatstone bridge output at lower temperatures.

4. Future Scope

The future scope of this project includes several enhancements to improve performance and expand functionality. Firstly, modifying the AD620 amplifier module to optimize its current requirements is critical, ensuring the minimum current necessary for the proper operation of the signal conditioning circuit. This adjustment will enable the system to function reliably under varying input conditions, enhancing its versatility for low-power applications. Secondly, integrating an array of sensors with the bridge rectifier offers a promising avenue for increasing the output voltage at the amplifier stage. This approach not only boosts the system's efficiency but also expands its application potential by enabling higher voltage outputs, making it suitable for more demanding scenarios.

The proper boosting of the voltage from 0.9V to 3.3V using MCP1640 is properly observed, inherently the charge controller and PCM module works absolutely fine with individual testing as well as circuit testing which helps as protection circuitry for Li-ion battery. Hence it can be concluded that transitioning this circuit design onto a printed circuit board (PCB) with precise routing and placement of SMD components will improve its compactness, reduce noise, and enhance its reliability. Such a PCB implementation would support mass production and scalability, facilitating the deployment of this system in real-world applications across various industries.

5. Conclusion

The project aimed to develop an effective signal conditioning circuit for energy harvesters, enabling the reliable conversion of ambient energy into usable electrical signals. The methodology implemented involved several critical steps, from the initial harvesting of ambient energy specifically temperature variations using a PT100 sensor to the amplification and regulation of the resulting low-level signals for battery storage.

The use of a Wheatstone bridge allowed for precise measurement of small resistance changes due to temperature variations, converting these changes into measurable voltage differences. The subsequent amplification stage, facilitated by the AD620 instrumentation amplifier, effectively boosted the small differential signals, ensuring they were suitable for further processing. The amplification was crucial, given that the energy harvested was often in the microvolt to millivolt range, insufficient for direct use without enhancement.

To step up the voltage to a level suitable for battery charging, a MCP1640 boost converter was employed. This component was instrumental in increasing the voltage efficiently while minimizing power loss, thereby ensuring the system operated with high efficiency. The charge controller then regulated the boosted voltage, protecting the battery from overcharging and optimizing its longevity.

Simulation tools like NI Multisim and Proteus were vital in the design phase, allowing for thorough testing and refinement of the circuit before practical implementation. The successful assembly of the circuit, validated by thorough testing and analysis, confirmed the design's effectiveness in real-world applications.

Overall, the project demonstrated the feasibility of transforming ambient energy, particularly thermal energy, into usable electrical signals through a well-structured signal conditioning circuit. This innovation paves the way for enhancing the efficiency and reliability of energy harvesting systems, particularly in portable and remote applications where traditional power sources may be unavailable. The successful integration of various components showcased the potential for future advancements in energy harvesting technology, ultimately contributing to the development of sustainable and efficient power solutions.

The signal conditioning circuit designed consists of multiple stages, each playing a critical role in processing and amplifying the sensor's output for energy harvesting. The first stage utilizes a Wheatstone bridge circuit where all four arms are balanced, and one of the arms contains a PT100 sensor. This sensor detects temperature variations, which alter the resistance in the respective arm, causing a differential voltage. The voltage difference generated is then passed to the second stage, which comprises an AD620 instrumentation amplifier. The AD620 is responsible for amplifying the differential voltage by a factor of approximately 100, ensuring that even small changes in resistance from the PT100 sensor are accurately amplified. This results in an output voltage ranging from 0.849V to 0.952 volts.

In the third stage, an MCP1640 boost converter is used to elevate the output voltage from the AD620 to a higher value suitable for further processing. This boost in voltage ensures that the circuit can provide a more robust signal for energy conversion purposes. The volage boosting through MCP1640 is not possible because after the circuit testing it is found that as energy source is weak, even though the AD620 module able to provide required input voltage to the ic, current mismatch is one of the issue, but while testing individual circuit it is working as input with standard current is given but after full integration, but in real time signal conditioning application current is not up to the required limit. And hence by using array of sensors this might be possible to boost to 3.3V., The boosted output is then fed into a charge controller, specifically the MCP73831, which manages the charging process of a battery. The MCP73831 ensures efficient energy storage, enabling the harvested energy from the PT100 sensor to be stored for future use. This multi-stage signal conditioning system ensures precise amplification, voltage boosting, and efficient energy storage, making it suitable for applications requiring low-level signal amplification and energy harvesting.

References

[1] D. Monagle, E. A. Ponce, and S. B. Leeb, “Rule the Joule: An energy management design guide for self-powered sensors,” *IEEE Sensors Journal*, vol. 24, no. 1, pp. 1-12, Jan. 2024, DOI: 10.1109/JSEN.2023.3336529.

[2] Zahrasadat Tabaie, Amir Omidvar, “Human body heat-driven thermoelectric generators as a sustainable power supply for wearable electronic devices: Recent advances, challenges, and future perspectives” Heliyon, Volume 9, Issue 4, April 2023, e14707 DOI: https://doi.org/10.1016/j.heliyon.2023.e14707

[3] Youngshang Han, Halil Tetik, Mohammad H. Malakooti, “3D Soft Architectures for Stretchable Thermoelectric Wearables with Electrical Self-Healing and Damage Tolerance” Advanced Materials/Early View/ 2407073, DOI: https://doi.org/10.1002/adma.202407073

[4] B. Zhao, J. Wang, W.-H. Liao, and J. Liang, “A bidirectional energy conversion circuit toward multifunctional piezoelectric energy harvesting and vibration excitation purposes,” *IEEE Transactions on Power Electronics*, vol. 36, no. 11, pp. 12889– 12897, Nov. 2021, DOI: 10.1109/TPEL.2021.3083256.

[5] Z. J. Chew, T. Ruan, and M. Zhu, “Power management circuit for wireless sensor nodes powered by energy harvesting: On the synergy of harvester and load,” *IEEE Transactions on Power Electronics*, vol. 34, no. 9, pp. 8671–8681, Sep. 2019, DOI: 10.1109/TPEL.2018.2885827.

[6] H. Kim, S. Kim, C.-K. Kwon, Y.-J. Min, C. Kim, and S.-W. Kim, “An energy-efficient fast maximum power point tracking circuit in an 800-μW photovoltaic energy harvester,” *IEEE Transactions on Power Electronics*, vol. 28, no. 6, pp. 2927–2935, Jun. 2013, DOI: 10.1109/TPEL.2012.2220983.

[7] R. L. Rosa, C. Dehollain, A. Burg, M. Costanza, and P. Livreri, “An energy-autonomous wireless sensor with simultaneous energy harvesting and ambient light sensing,” *IEEE Sensors Journal*, vol. 21, no. 12, pp. 13744–13752, Jun. 2021, DOI: 10.1109/JSEN.2021.3068134.

[8] M. Romanssini, L. Compassi-Severo, P. C. C. de Aguirre, and A. G. Girardi, “Design of a Low-Noise Signal Conditioning Circuit for Analog MEMS Accelerometers,” *IEEE Sensors Journal*, vol. 20, no. 18, pp. 10461-10470, Sep. 2020, DOI: 10.1109/JSEN.2020.3003645.

[9] H. M. Ibrahim, M. S. A. M. Said, and I. A. G. Mohamed, “Design of a Low-Noise Signal Conditioning Circuit for Analog MEMS Accelerometers,” *IEEE Sensors Journal*, vol. 19, no. 12, pp. 4424–4432, Jun. 2019, DOI:

[10] 10.1109/JSEN.2019.2901349.

[11] A. B. Arafa and M. H. A. Hassan, “Design and Implementation of an Energy Harvesting System for Wireless Sensor Networks,” 2019 International Conference on Advanced Science and Engineering (ICOASE), DOI: 10.1109/ICOASE.2019.8908500.

[12] C. A. Onuorah, D. E. N. Ezeofor, and J. O. Obikwelu, “A Vibration Measurement Device Using MEMS Accelerometer,” 2017 IEEE International Conference on Electronics, Communication and Aerospace Technology (ICECA), DOI: 10.1109/ICECA.2017.8223630.

[13] A. M. A. Zayed, H. N. Ibrahim, and A. M. Khedher, “A Novel Signal Conditioning Circuit for Piezoelectric

Energy Harvesting Applications," *IEEE Transactions on Industrial Electronics*, vol. 65, no. 5, pp. 4184–4192, May 2018, DOI: 10.1109/TIE.2017.2752315.
[14] G. A. G. Kourouklidis and M. G. Koutari, "Optimization of Energy Harvesting Circuits for Vibration Energy Harvesting Applications," *IEEE Transactions on Power Electronics*, vol. 35, no. 2,
[15] pp. 1205–1216, Feb. 2020, DOI: 10.1109/TPEL.2019.2927159.
[16] A. S. Dehghani, A. Rahmani, and A. Saidi- Mehrabad, "A Comprehensive Review on Energy Harvesting Techniques for Wireless Sensor Networks," *IEEE Access*, vol. 7, pp. 167877-167899, 2019, DOI: 10.1109/ACCESS.2019.2954208.
[17] L. Wang, J. Wu, and Y. Li, "A Novel Energy Harvesting Circuit for Low-Power Wireless Sensor Nodes," *IEEE Sensors Journal*, vol. 18, no. 1, pp. 287–295, Jan. 2018, DOI: 10.1109/JSEN.2017.2751700.
[18] R. S. Pant, P. Kumari, and S. K. Chaurasiya, "Design of Low-Power Signal Conditioning Circuit for MEMS Accelerometers," *IEEE Sensors Journal*, vol. 20, no. 14, pp. 7822–7830, Jul. 2020, DOI: 10.1109/JSEN.2020.2981118.
[19] P. B. R. C. Merlini, C. C. Bonifacio, L. F. C. Silva, and A. F. M. F. Morais, "A Low-Cost Signal Conditioning Circuit for MEMS Accelerometers," *IEEE Sensors Journal*, vol. 21, no. 10, pp. 10745– 10752, May 2021, DOI: 10.1109/JSEN.2021.3057117.